Eduvest - Journal of Universal Studies
Volume 5 Number 5, May, 2025
p- ISSN 2775-3735- e-ISSN 2775-3727

ASSESSING FLOOD DISCHARGE DYNAMICS IN SURAKARTA THROUGH LAND COVER MAPPING WITH SENTINEL-2A

Fridya Ikafitri N*, Rr Rintis Hadiani, Ali Rahmat
Universitas Sebelas Maret, Indonesia
Email: fridyaikafitri17@student.uns.ac.id, rintis@ft.uns.ac.id, alirahmat@pu.go.id

ABSTRACT

Rapid urbanization in Surakarta, Central Java, has transformed land cover, reducing water absorption capacity and increasing flood frequency. While global studies link land cover changes to flood risks, localized analyses in Surakarta remain scarce. This study aims to (1) map land cover changes (2019–2023) using Sentinel-2A imagery, (2) quantify their impact on runoff coefficients and flood discharge, and (3) evaluate classification accuracy against government data. Land cover was classified via MLC (97% accuracy) and validated against BPS and Ministry of Environment and Forestry data. Hydrological modeling combined HSS Gama I and SCS methods in HEC-HMS, with rainfall data analyzed using Thiessen polygons and Gumbel distribution. Urbanization increased the runoff coefficient by 23.12%, raising flood discharge by 23.47% (Gajah Putih) and 23.33% (Pepe Hulu). Sentinel-2A outperformed government data (79% accuracy) in land cover mapping. The findings underscore the urgency of integrating high-accuracy remote sensing into urban planning. Future research should explore machine learning for real-time flood prediction and policy-driven mitigation strategies.

Keywords *Sentinel-2A; the dynamics of flood discharge; Factor*

Article Info:
Submitted: 23-04-2025 Final Revised: 14-05-2025 Accepted: 20-05-2025 Published: 20-05-2025

INTRODUCTION

The city of Surakarta is known as one of the urbanization centers in Central Java that has undergone significant land changes due to the rapid urbanization and industrialization process (Wahyudi et al., 2020). Urbanization significantly increases flood risk by changing land use and cover, increasing discharge, and peak flood volume. For example, in Beijing, urban land cover increased from 25.22% to 65.48%, resulting in a 7.02% increase in floodplain discharge (Kabeja et al., 2022). In transitional watersheds, projections show that urban areas will develop significantly with an increase in peak discharge of 5% and 6.8% for future storm

How to quote: Ikafitri N, F., Hadiani, R. R., & Rahmat, A. (2025). Assessing Flood Discharge Dynamics in Surakarta Through Land Cover Mapping with Sentinel-2A. Eduvest Journal. *5*(5): 5091-5107.
E-ISSN: 2775-3727
Published by: https://greenpublisher.id/

events it is necessary to regulate land-use changes (Handayani, 2022; Larasati et al., 2022; Subkhi & Mardiansjah, 2019).

This transformation is mainly characterized by a reduction in water catchment areas and an increase in watertight surfaces, such as concrete and asphalt, that disrupt the hydrological balance and increase the risk of flooding (Bachmid F & Ariyanto, 2017; Sudiana, Rovara, et al., 2019; Sudiana, Umbara, et al., 2019). Data from the Surakarta Regional Disaster Management Agency (BPBD) shows that the frequency of floods has increased significantly in the last ten years, with areas such as Banjarsari and Laweyan Districts being the most vulnerable to flood impacts (BPBD Surakarta, 2022).

Floods are a natural disaster often occurring in various regions, including Surakarta. This phenomenon causes material losses, threatens life safety, and disrupts community activities. One factor affecting the dynamics of flooding is changes in land cover due to urbanization, land conversion, and other human activities. Global findings that land use change is a significant factor in increased surface *runoff* and flood discharge (Fletcher et al., 2013; Weng, 2021)

Remote sensing technology, such as the Sentinel-2A satellite imagery, was launched by a collaboration between *the European Commission and the European Space Agency* in the *Global Monitoring for Environment and Security* (GMES) program. The Sentinel-2A satellite provides an opportunity to accurately and sustainably monitor land cover changes (ESA, 2023). Previous studies, such as those conducted by Dewan & Corner (2014) in Dhaka and Li et al (2020) in Shanghai, have proven the effectiveness of Sentinel-2A data in mapping the relationship between urbanization and increased flood discharge. However, similar research has never been conducted in the city of Surakarta, even though the rate of land change is among the highest in Central Java Province (BPS, 2023)

Geographic Information Systems (GIS) are used for spatial mapping and analysis. The integration of Sentinel 2-A satellite data with GIS spatial analysis allows for more accurate and real-time mapping of flood-prone areas (Falah et al, 2020). For the analysis of flood discharge, this study integrates the HSS Gama I and HSS SCS methods. HSS Gama I, developed specifically for tripis conditions (Harto, 1993), will be combined with spatial parameters such as slope, soil type, and land cover obtained from GIS mapping. Meanwhile, the SCS method with the Curve Number (CN) parameter will be calculated based on the land cover map resulting from the classification of Sentinel-2A imagery (USDA, 1986). This combination allows for more precise modeling of flood discharge by considering the spatial characteristics of the Bengawan Solo watershed in the Surakarta area.

Several recent studies have demonstrated the effectiveness of GIS integration and remote sensing for flood analysis. Research by (Kurniawan et al., 2022) in Semarang succeeded in mapping flood inundation areas with 85% accuracy using Sentinel-2A and DEM (*Digital Elevation Model*). Meanwhile, Liu developed a spatial model for urban flood prediction based on *Shanghai's machine learning and GIS data*.

Changes in land cover due to urbanization and land conversion can affect flood discharge, ultimately increasing the risk of flooding in Surakarta. Therefore, accurate land cover mapping and in-depth analysis of their impact on flood

discharge are essential for effective flood risk management. With proper mapping, we can identify the most vulnerable areas to flooding and plan appropriate mitigation measures. In the study, Sentinel-2A satellite imagery was used to create highly detailed land cover maps. These maps are critical to predicting future flood risks and supporting better urban development planning (Nguyen et al., 2021).

This study aims to analyze the dynamics of flood discharge in Surakarta through land cover mapping using Sentinel-2A imagery. This study advances existing research by (1) focusing specifically on Surakarta, a rapidly urbanizing city in Central Java, which has not been extensively studied in the context of land cover-flood dynamics despite its high flood risk (BPBD Surakarta, 2022; BPS, 2023). Unlike prior studies in Dhaka (Dewan & Corner, 2014) or Shanghai (Li et al., 2020), it integrates Sentinel-2A imagery with the Maximum Likelihood Classification (MLC) method, achieving 97% accuracy—higher than the Ministry of Environment and Forestry's 79%—and validating results with local BPS data, thus addressing discrepancies in land cover classification. (2) It uniquely combines HSS Gamma I and SCS methods in HEC-HMS to model flood discharge, capturing localized hydrological responses in the Gajah Putih and Pepe Hulu watersheds, which were previously unanalyzed. (3) The study quantifies a 23.12% increase in runoff coefficients (2019–2023), directly linking urbanization to flood risk escalation, a granular insight absent in broader regional studies (Kabeja et al., 2022). (4) It proposes machine learning integration for future flood prediction, building on but extending beyond traditional GIS-based approaches (Kurniawan, 2022; Liu, 2021).

RESEARCH METHODS

This research is in Surakata City, covering the Banjarsari District, Jebres District, Laweyan District, Pasar Kliwon District, and Kecamatan Serengan. The river system in Surakarta City consists of 8 main channels, including Kali Anyar, Kali Pepe Hilir, Kali Pepe Hulu, Kali Gajah Putih, Kali Pelem Wulung-Kali Brojo-Kali Tanggul, Kali Jenes, Kali Wingko, and Kali Boro.

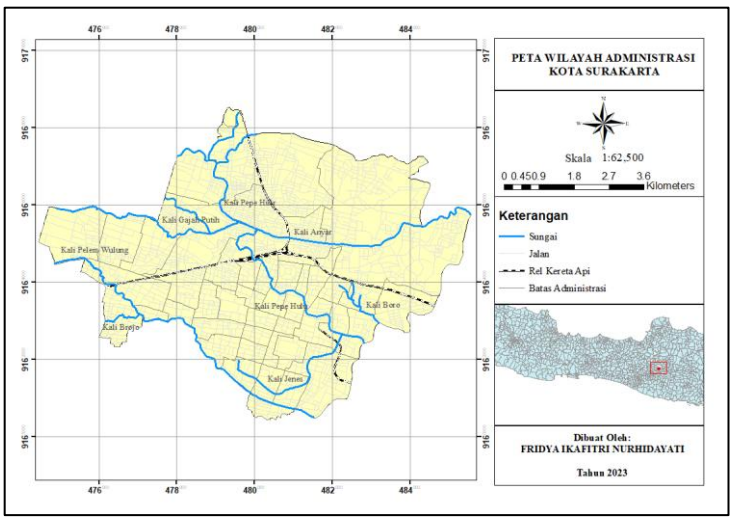

Figure 1. Surakarta City Administration Map

Research Tools and Materials

In this study, secondary data were used, including

1. Rain Station Data from 2004 to 2023. PSDA B.Solo Office Station, Pabelan Station, Grogol Station, and BPSDA Station were obtained from the Central Java Water Resources and Spatial Planning Center and the Bengawan Solo River Basin Organization
2. Surakarta City Administration Map
3. Sentinel 2-A Satellite Images in 2019 and 2023
4. Land Cover Map sourced from the Ministry of Environment and Forestry (MoEF)
5. Statistical data on land cover change in the city of Surakarta in 2019

The tools used in this study include

1. HEC-HMS for flood discharge simulation
2. GIS to process complex images, create watersheds
3. *Microsoft Excel* for data processing and analysis

Land Cover Analysis

In this study, the Sentinel-2A image processing process uses the Maximum Likelihood classification method as the main technique for land cover mapping. This method was chosen because of its ability to distinguish objects based on spectral characteristics with a high degree of accuracy (Richards & Jia, 2006). The Maximum Likelihood method has been proven effective for land cover classification in urban areas with an accuracy of up to 85-90% (Zhang et al., 2021). The image processing process will go through the main stages:

1. Sentinel-2A Satellite Image Download
   Figure 2 shows the steps taken to download Sentinel-2A satellite image data through the official Google Earth Engine page.

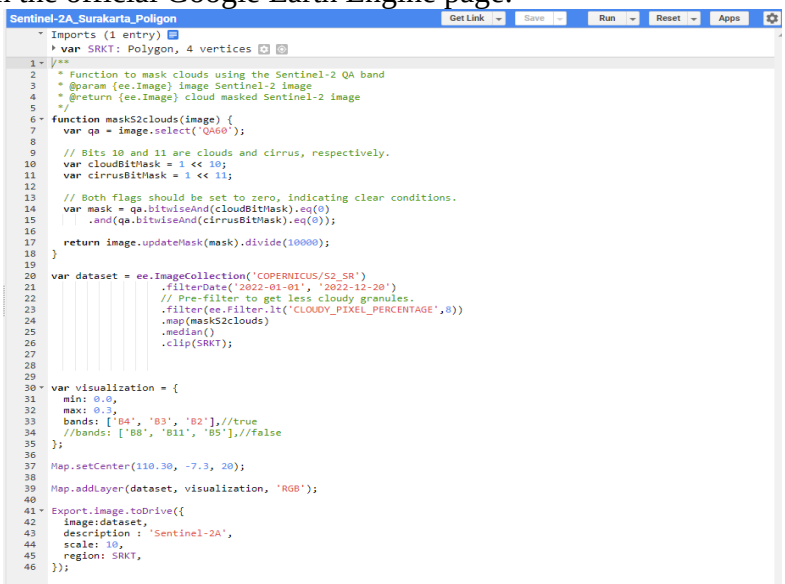

Figure 2. Satellite Image Download Code Script

2. *Preprocessing*
   Sentinel-2A imagery downloaded through *Google Earth Engine* has been radiometrically and atmospherically corrected using sen2cor. With a low cloud presence rate of 8%, no additional cloud masking processing is required. The image resolution has been equalized to 10 meters, so resampling is no longer needed.
3. Sample Taking Level to SNI 7645-2010
   The calculation of the number of samples in this land cover classification is determined based on the Slovin formula in Sugiyono (2017) with a confidence level of 95%, with a value of e = 0.05, which can be seen in the following formula

$$n = \frac{\mathrm{N}}{1 + Ne^2}$$

information:

n	= Number of samples sought
N	= Number of pixels of the study population
e	= A 5% error rate

4. The Accuracy Test Level is calculated according to Jensen (2005) in Lillesand & Kiefer (1994) with the following equations:

$$\text{User Accuracy (\%)} = \frac{\mathrm{V}}{\mathrm{V+K}} \text{ X } 100\%$$

$$\text{Producer Accuracy (\%)} = \frac{\mathrm{V}}{\mathrm{V+O}} \text{ X } 100\%$$

$$\text{Overall Accuracy (\%)} = \frac{\mathrm{V}}{\mathrm{V+O+K}} \text{ X } 100\%$$

$$\text{Accuracy (\%)} = \frac{\mathrm{N}\ \Sigma_{\mathrm{i}}^{\mathrm{r}} X\ x_i^i - \Sigma_{\mathrm{i}}^{\mathrm{r}} x_i + x + i}{N^2 - \Sigma_{\mathrm{i}}^{\mathrm{r}}\ x_i + x + i} \text{ X } 100\%$$

information:

V	= Data valid
O	= Omission error data
K	= Commission error data
N	= Number of pixels in the example
X	= Diagonal value of the contingency matrix
Xii	= Number of pixels in row to i
Xi+	= Number of pixels in column to i

The degree of conformity of kappa coefficient values according to can be seen in the following table:(Congalton RG., 1999)

Table 1. Kappa Suitability Rate

Suitability Rate (%)	Confidence Level
>40	Low
50-80	Keep
>80	Tall

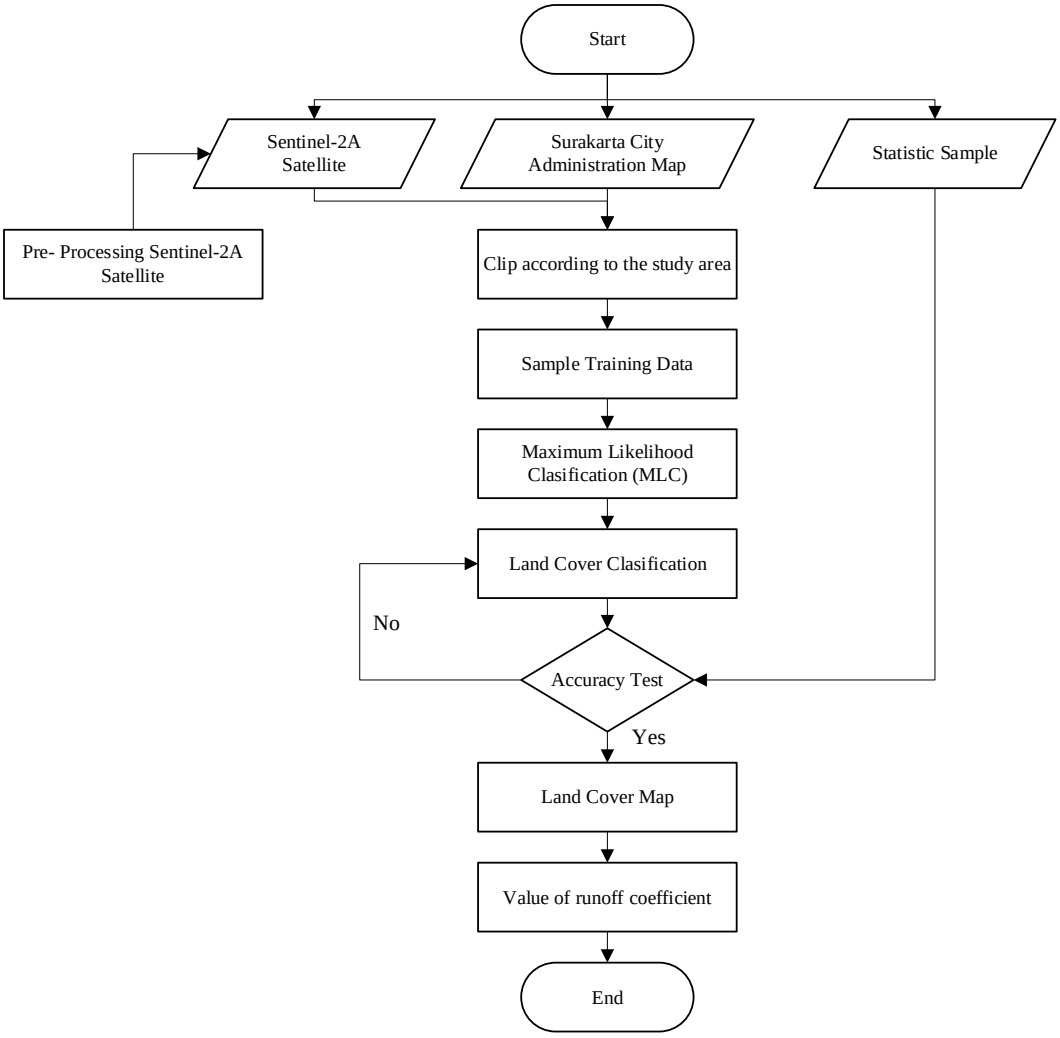

Figure 3. Land Cover Analysis Flow Chart Diagram

Hydrological Analysis

1. Consistency Test

   The *Double Mass Curve* method is used to detect inconsistencies in rain data by comparing the accumulation of data from the station to be tested with the accumulation of data from other stations. The data is considered inconsistent if there is a graph tilt (Searcy & Hardison, 1960). In addition to the double mass

curve method, the data concurrency can be tested using *the Rasch-adjusted partial Sums* (RAPS) method. This method aims to identify systematic changes in hydrological data by analyzing the average cumulative deviation (Vogel & Kroll, 1989).

2. Rain Region
   Calculating regional rainfall using the Thiessen polygon method by giving the appropriate weight based on the area of influence of each nearest rain station (Thiessen, 1911; Asdak, 2010).
3. Distribution Types
   The selection of appropriate statistical distributions, such as Normal, Normal Log, Gumbel, and log-Pearson II, is very important in frequency analysis (Chow, 1988; Soewarno, 1995). Therefore, the selection of distribution types is very important in frequency analysis to accurately model rainfall and discharge data (Kurniawan & A.R., 2021).
4. Spread Match Test
   Distribution Match tests, such as *Smirnov-Kolmogorov* and *Chi-square*, are used to determine whether the data obtained follows a specific type of distribution (Ahmad & A.R., 2020)
5. Coefazine Limpasan
   The runoff coefficient (Curve Number) calculates the proportion of rain that turns into surface flow. The value of this coefficient is influenced by various factors, namely land use, urbanization, and soil conditions.
6. Flood Discharge Analysis
   The HSS Gama I method is used in flood discharge analysis to calculate unit hydrographs by considering the characteristics of the watershed so that it can provide a more accurate estimate of flood potential (Sari & Rahman, 2020). The HSS SCS (Soil Conservation Service) method uses the curve number model in the HEC-HMS software. This model estimates excess precipitation based on cumulative rainfall, land cover, and land use integrated in HEC-HMS to produce a more accurate estimate of surface flow (Indra Nurdianto, 2023)

RESULTS AND DISCUSSION

Land Cover Analysis

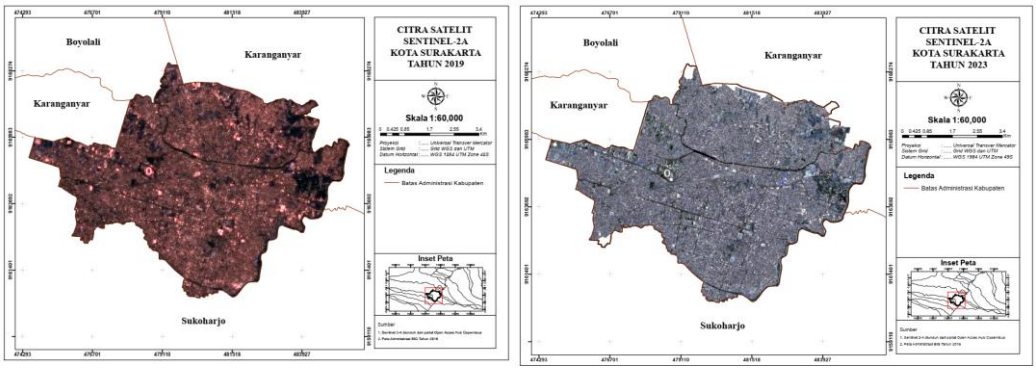

Figure 4. Sentinel-2A Satellite Imagery for 2019 and 2023

The intake training sample refers to SNI 7645-2010, where land cover was classified using a thorough and random sampling method. Below are the selected sample areas.

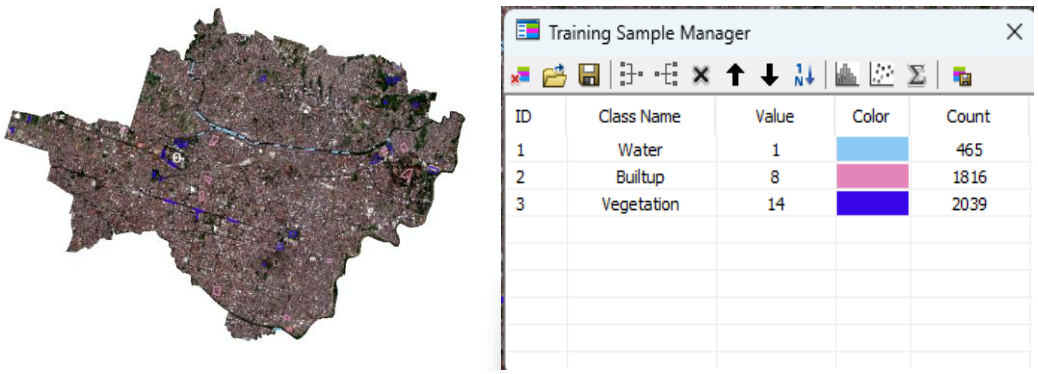

Figure 5. Training Sample: Taking Pictures

MLC classification results

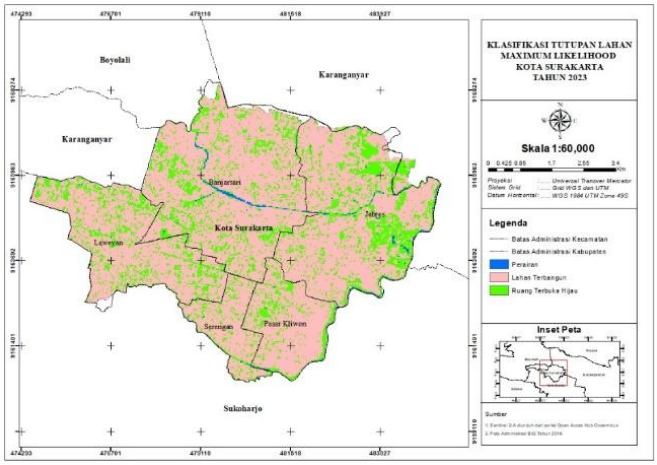

Figure 6. MLC Classification Results in 2023

The results of MLC processing of Sentinel 2A satellite imagery with the classification of land cover in the form of waters, built-up land, and green open space with an area in 2023 can be seen in the following Table 2

Table 2. Surakarta City Land Cover Area Table in 2023

Yes	Land Cover	Area (Ha)	Percentage(%)
1	Waters	36.93	0.80
2	Built Land	3546.62	76.72
3	Green Open Space	1039.05	22.48
	Total Area	4622.60	100

Accuracy Test Results

Table 3. Accuracy Test Results in 2023

	Objek	Building	RTH	Waters	Sum	*User's Accuracy* (%)
Processing Data	Building	19	1	0	20	95
	RTH	3	17	0	20	85
	Waters	1	1	18	20	90
	Sum	23	19	18	60	
Producer Accuracy (%)		82.6	89.4	100		
Overall Accuracy (%)			90			
Kappa Accuracy (%)			85			

The results of the 2023 accuracy test show an *Overall Accuracy value* of more than 90%. This indicates that the land cover classification results are 90% in accordance with the actual conditions in the field. Kappa Accuracy has an accuracy of more than 85%, which refers to the level of conformity of the kappa coefficient at high grade values.

Value of Runoff Coefficient (*Curve Number*)

Land cover is related to flood discharge through the runoff coefficient (curve number) value, which reflects how much of the rain changes to surface flow. Changes in land cover, such as urbanization or deforestation, can increase the value of runoff coefficients, thereby increasing flood discharge. The following is the value of runoff coefficients from several land cover maps.

Table 4. Recapitulation of Land Cover Value

No	Land Cover Map	Year	CN
1	MoEF	2019	0.91859
2	MoEF	2020	0.91932
3	MoEF	2022	0.91932
4	Citra Sentinel-2A	2019	0.68948
5	Citra Sentinel-2A	2022	0.84403
6	Citra Sentinel-2A	2023	0.84871

The runoff coefficient (CN) values of the Sentinel-2A image increased from 2019 to 2023, indicating an increase in surface potential. This is very important to consider in hydrological analysis and water resource management.

Hydrological Analysis

1. Rain Data Consistency Test

- Double Mass Curve Method

Annual cumulative rainfall data were tested for consistency using the double mass curve method by comparing two data sets. The data is considered consistent if the determination value (R2) is close to 1.

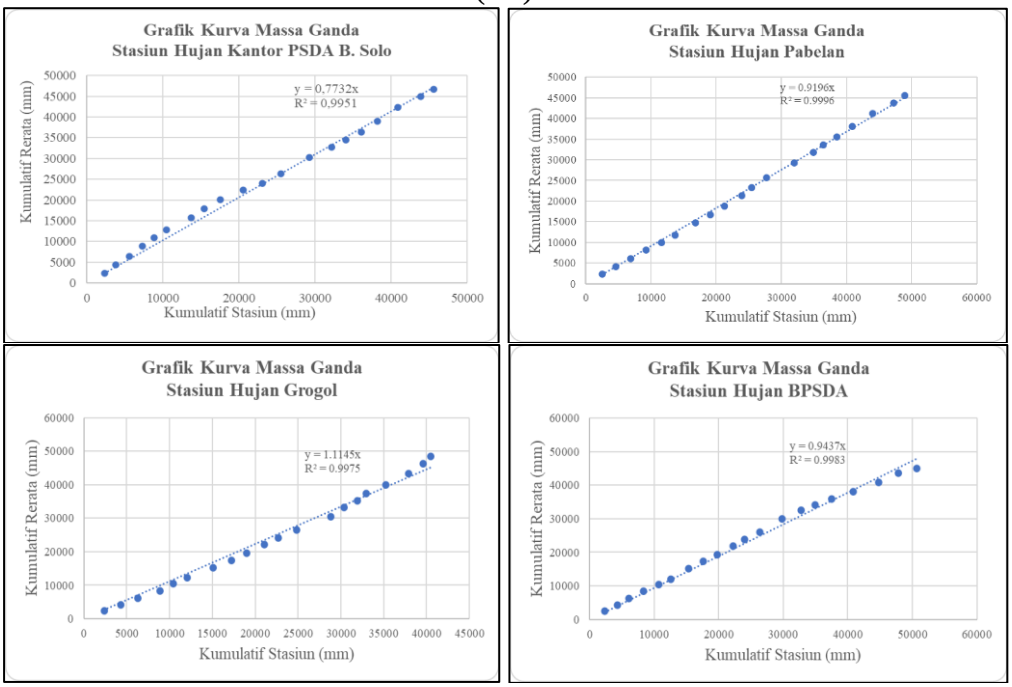

Figure 7. Double Mass Curve Graph

Figure 7 shows the relationship between the cumulative PSDA B.Solo Office Station, Pabelan Station, Grogol Station, and BPSDA Station, which forms an almost straight line. Each station has a coefficient of determination that is close to 1. So that it can be concluded that the data used is consistent

- RAPS Method

Table 5. RAPS Method Data Consistency Test

Rain Station	$Q/n^{0.5}$	$R/n^{0.5}$	Information
	1.22	1.43	
Sta. PSDA B.Solo	0.860	1.191	Homogeneous
Sta. Pabelan	0.494	0.839	Homogeneous
Sta. Grogol	0.604	1.204	Homogeneous
Sta. BPSDA	0.676	1.110	Homogeneous

Based on the calculations in Table 5, the values $Q/n^{0.5}$ and R/n0.5 were compared to the critical value with n = 20, and the confidence interval was 95%. So, the results of the comparison of the Q_{RAPS} value and the critical value, which is less than 1.22, show that the rain data is homogeneous. The results of the comparison of the R_{RAPS} and the critical value of less than 1.43 showed that the rain data were homogeneous.

2. Calculation of Region Rainfall: Thiessen Polygon Method

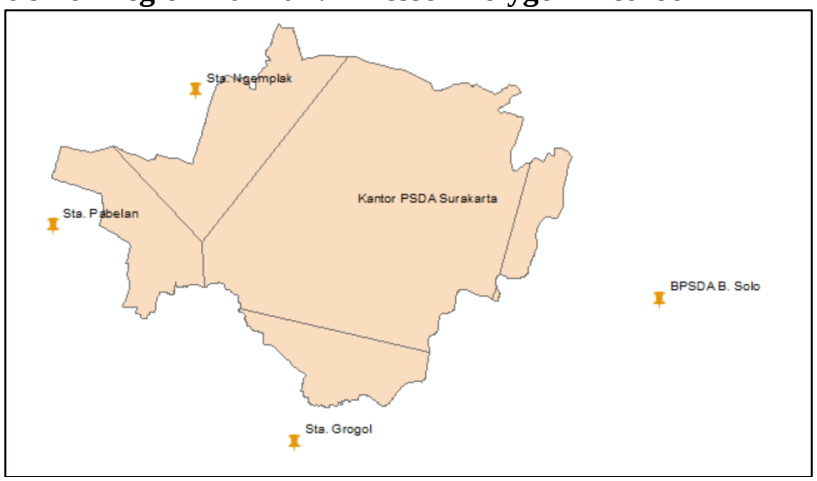

Figure 8. Thiessen Polygon Analysis Images

Table 6. Thiessen Coefficient Values

No	Rain Station	Area (A)	Koefisien *Thiessen*	%
		km²	(Kr)	
1	Sta. PSDA B.Solo	28.6380	0.6135	61.3470
2	Sta. Pabelan	4.9300	0.1056	10.5608
3	Sta. Grogol	4.1200	0.0883	8.8257
4	Sta. BPSDA	1.9160	0.0410	4.1044
5	Sta. PSDA B.Solo	7.0780	0.1516	15.1622
	Total DAS Moons	46.6820	1	100

The calculated Thiessen *coefficient* is then used to find the region's rainfall. The results of the recapitulation of the rain calculation of the review area of the PSDA B.Solo Kantro Station, Pabelan Station, Grogol Station, BPSDA Station, and Ngemplak Station.

3. Rain Distribution Analysis

The rainfall distribution is analyzed based on regional rainfall. This study uses the Normal Distribution Method, Normal Log Distribution, Gumbel Distribution, and Pearson Log Distribution III.

Table 7. Statistical Parameters for Determination of Distribution Type

No	Distribution Type	Parameters Statistics			Information
		Cs	Ck	Cv	
1	Normal Distribution	0.49	2.33	0.24	Not Compliant
2	Normal Log Distribution	0.25	2.05	0.06	Not Compliant
3	Gumbel Distribution	0.49	2.33	0.24	Not Compliant
4	Pearson III Log Distribution	0.25	2.05	0.06	

4. Distribution Compatibility Test

- Smirnov Kolmogorov Test

For the amount of as many as 20 rainfall data and the degree of confidence (α) of 5%, a critical ΔP value of 0.290 was obtained. Recapitulation of Maximum ΔP and Critical ΔP values of each method in Table 8

Table 8. Comparison of ΔP max and critical ΔP

Result	Normal	Log Normal	Gumbel	Log Pearson III
DP max	0.151	0.134	0.0995	0.1120
Δp is critical	0.290	0.290	0.290	0.290
Hypothesis	ACCEPTED	ACCEPTED	ACCEPTED	ACCEPTED

- Chi-Square Test

Table 9. Comparison of X^2 and X^2cr

Result	Normal	Log Normal	Gumbel	Log Pearson III
X^2	5.167	13.000	6.800	10.467
X^2_{cr}	7.180	7.180	7.180	7.180
Hypothesis	ACCEPTED	REJECTED	ACCEPTED	REJECTED

After analyzing the Smirnov-Kolmogorov and Chi-Square Tests on each Normal Probability Distribution, Normal Log, Gumbel, and Log Pearson III, it can be concluded that the distribution method that meets is the Gumbel Probability Distribution.

5. Hydrograph Calculation of Synthesis Units

In the hydrographic analysis, the synthesis unit is more focused on the Gajah Putih and Pepe Hulu watersheds in the city of Surakarta. Its location in Banjarsari District is one consideration because floods often occur in the sub-district. This analysis aims to provide a more accurate picture of the area's hydrological response to help in planning and managing water resources more effectively.

The HSS SCS analysis used HEC-HMS software version 4.10 to calculate the runoff coefficient (CN) value. The stages of discharge calculation include making a basin model, entering ABM distribution data each year for each sub-watershed, and running simulations.

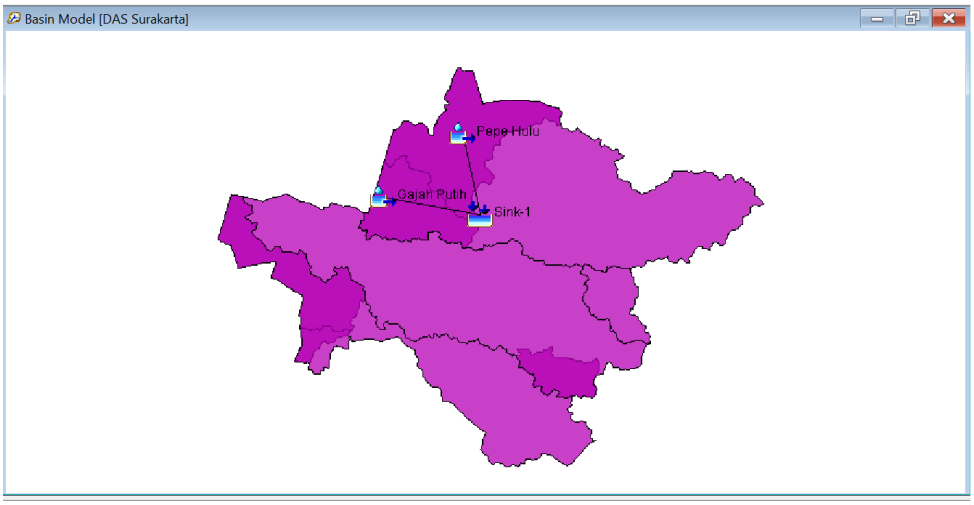

Figure 9. Basin Model HEC-HMS

In the hydrographic analysis of the synthesis unit, two conditions were used, namely the first condition using the curve number value obtained from the 2019 Sentinel-2A image classification and the second condition using the CN value from the 2023 Sentinel-2A image classification. This approach is carried out to determine the discharge change over that time. The recapitulation of the results of the analysis of the HSS Gama I and HSS SCS calculations is in Table 10.

Table 10. Recapitulation of Flood Discharge Calculation Results in the Gajah Putih and Pepe Hulu Rivers

No	Years	Condition 1 (runoff coefficient 2019) Discharge (m^3/dtk)				Condition 2 (runoff coefficient 2023) Discharge (m^3/dtk)			
		HSS Gamma 1		HSS SCS		HSS Gamma1		HSS SCS	
		Gajah Putih	Pepe Hulu	Gajah Putih	Pepe Hulu	Gajah Putih	Pepe Hulu	Gajah Putih	Pepe Hulu
1	2004	11.50	15.48	17.7	30.9	13.63	18.64	21.8	38
2	2005	10.82	14.47	16.4	28.6	12.78	17.39	20.2	35.2
3	2006	9.97	13.20	14.8	25.7	11.73	15.82	18.1	31.6
4	2007	18.17	25.39	30.5	53.2	21.83	30.84	37.6	65.5
5	2008	17.06	23.74	28.4	49.5	20.47	28.81	34.9	60.9
6	2009	15.33	21.18	25.1	43.7	18.34	25.65	30.8	53.8
7	2010	11.59	15.61	17.9	31.1	13.73	18.80	22	38.3
8	2011	10.10	13.40	15	26.2	11.90	16.07	18.5	32.2
9	2012	12.53	17.02	19.6	34.3	14.90	20.53	24.2	42.2
10	2013	10.64	14.19	16	27.9	12.56	17.05	19.7	34.4
11	2014	17.07	23.77	28.4	49.5	20.48	28.84	35	61
12	2015	13.83	18.94	22.2	38.7	16.49	22.89	27.3	47.6
13	2016	11.23	15.07	17.2	30	13.28	18.13	21.1	36.8
14	2017	14.22	19.52	22.9	40	16.97	23.61	28.2	49.2
15	2018	10.53	14.03	15.8	27.6	12.42	16.85	19.5	33.9
16	2019	14.75	20.31	23.9	41.7	17.62	24.58	29.5	51.4
17	2020	12.15	16.44	18.9	33	14.42	19.82	23.3	40.6
18	2021	15.23	21.02	24.9	43.4	18.21	25.46	30.6	53.4
19	2022	15.43	21.32	25.2	44	18.46	25.82	31.1	54.2
20	2023	10.57	14.10	15.9	27.7	12.48	16.93	19.6	34.1

CONCLUSION

The study found that land cover changes from 2019 to 2023 significantly increased runoff coefficients by 23.12%, reducing water absorption capacity and raising flood risks, with flood discharge rising by 23.47% in the Gajah Putih watershed and 23.33% in the Pepe Hulu watershed. Sentinel-2A satellite imagery processed with the MLC method (97% accuracy) provided more reliable land cover data than the Ministry of Environment and Forestry (79% accuracy), aligning closely with BPS Surakarta. Future research should explore urban planning strategies to mitigate runoff, standardize land cover classification, integrate climate projections into flood modeling, assess socioeconomic and ecological impacts, and leverage machine learning for improved land cover and flood prediction systems.

REFERENCE

Ahmad, M. S., & A. R. (2020). Analisis uji kecocokan sebaran curah hujan menggunakan metode Kolmogorov-Smirnov dan Chi-Square. *Jurnal Meteorologi dan Geofisika, 8*(2), 89–95.

Asdak, C. (2010). *Hidrologi dan Pengelolaan Daerah Aliran Sungai*. Gadjah Mada University Press.

Bachmid, F., & Ariyanto. (2017). Strategi Penanganan Kawasan Permukiman Kumuh Kota Ternate. *Jurnal Plano Madani, 6*(2).

BPBD Surakarta. (2022). *Laporan Tahunan Kejadian Bencana Kota Surakarta*.

BPS. (2023). *Statistik Daerah Kota Surakarta 2023*. Badan Pusat Statistik.

Chow, V. T., Maidment, D. R., & Mays, L. W. (1988). *Applied Hydrology*. McGraw-Hill.

Congalton, R. G. (1999). Accuracy assessment and validation of remotely sensed data: Principles and practices. In S. Morain & S. L. Baros (Eds.), *Remote sensing for sustainable ecosystem management* (pp. 125–142). Lewis Publisher.

Dewan, A. M., & Corner, R. J. (2014). Impact of Land Use/Cover Changes on Flooding in Dhaka, Bangladesh. *International Journal of Applied Earth Observation and Geoinformation, 31*, 45–55.

ESA. (2023). *Sentinel-2 User Handbook*. European Space Agency.

Falah, F., et al. (2020). GIS-Based Spatial Modeling of Flood Risk Areas in Iran. *Geomatics, Natural Hazards and Risk, 11*(1), 231–251.

Fletcher, T. D., et al. (2013). Understanding, Management, and Modelling of Urban Hydrology and Its Consequences for Receiving Waters. *Water Research, 47*(14), 4791–4801.

Handayani, S. A. (2022). Bibliografi Sejarah Perkotaan: Dari Kota Tradisional sampai Modern. *Historia, 5*(2). https://doi.org/10.19184/jh.v5i2.36314

Harto, S. (1993). *Analisis Hidrologi*. PT Gramedia Pustaka Utama.

Indra Nurdianyoto. (2023). *Analisis Hujan - Debit Banjir Menggunakan Model HEC-HMS*. Universitas Brawijaya.

Jensen, J. R. (2005). *Introductory digital image processing: A remote sensing perspective* (3rd ed.). Prentice Hall.

Kabeja, C., Li, R., Rwatangabo, D. E. R., & Duan, J. (2022). Monitoring Land Use/Cover Changes by Using Multi-Temporal Remote Sensing for Urban Hydrological Assessment: A Case Study in Beijing, China. *Remote Sensing*.

Kurniawan, K. A. M. S., & A. R. (2021). Pemilihan distribusi sebaran curah hujan menggunakan metode statistik di wilayah Sungai Brantas. *Jurnal Teknik Sipil*, *12*(3), 67–75.

Kurniawan, R. (2022). Flood Mapping Using Sentinel-2 and GIS in Coastal Cities. *International Journal of Disaster Risk Reduction*, *67*, 102689.

Larasati, A. P., Rahman, B., & Kautsary, J. (2022). Pengaruh Perkembangan Perkotaan terhadap Fenomena Pulau Panas (Urban Heat Island). *Jurnal Kajian Ruang*, *2*(1). https://doi.org/10.30659/jkr.v2i1.20469

Li, X., et al. (2020). Urbanization-Induced Land Use Change Increases Flood Risk in Shanghai. *Journal of Hydrology*, *590*, 125364.

Lillesand, T. M., & Kiefer, R. W. (1994). *Remote sensing and image interpretation* (3rd ed.). Wiley.

Liu, W. (2021). Machine Learning-Based Urban Flood Modeling. *Journal of Hydrology*, *603*, 126989.

Nguyen, H. D., Fox, D., Dang, D. K., Pham, L. T., Du, Q. V. V., Nguyen, T. H. T., Dang, T. N., Tran, V. T., Vu, P. L., Nguyen, Q.-H., Nguyen, T. G., Bui, Q.-T., & Petrisor, A.-I. (2021). Predicting Future Urban Flood Risk Using Land Change and Hydraulic Modeling in a River Watershed in the Central Province of Vietnam. *Remote Sensing*, *13*(2), 262.

Richards, J. A., & Jia, X. (2006). *Remote Sensing Digital Image Analysis*. Springer.

Sari, D., & Rahman, A. (2020). Analisis Debit Banjir Menggunakan Metode HSS Gama 1. *Jurnal Hidrologi*, *12*(1), 45–56.

Searcy, J. K., & Hardison, C. H. (1960). *Double-Mass Curves*. USGS Water-Supply Paper 1541-B.

Soewarno, S. (1995). *Hidrologi Aplikasi Metode Statistik untuk Analisis Data*. Nova.

Subkhi, W. B., & Mardiansjah, F. H. (2019). Pertumbuhan dan Perkembangan Kawasan Perkotaan di Kabupaten: Studi Kasus Kabupaten Sleman, Daerah Istimewa Yogyakarta. *Jurnal Wilayah Dan Lingkungan*, *7*(2). https://doi.org/10.14710/jwl.7.2.105-120

Sudiana, N., Rovara, O., & Astisiasari, A. (2019). Analisis Potensi Bahaya Bencana Kebakaran Perkotaan di Provinsi DKI Jakarta. *Jurnal Sains Dan Teknologi Mitigasi Bencana*, *13*(2). https://doi.org/10.29122/jstmb.v13i2.2904

Sudiana, N., Umbara, R. P., & Zahro, Q. (2019). Kajian Kapasitas Daerah Terhadap Bencana Kebakaran Perkotaan (Studi Kasus di Kecamatan Cakung, Kota Jakarta Utara). *Jurnal Sains Dan Teknologi Mitigasi Bencana*, *13*(1). https://doi.org/10.29122/jstmb.v13i1.2910

Sugiyono. (2017). *Metode Penelitian Bisnis (Pendekatan Kuantitatif, Kualitatif, Kombinasi dan R&D)*. In *Metodelogi Penelitian*.

Thiessen, A. H. (1911). Precipitation averages for large areas. *Monthly Weather Review*, *39*(7), 1082–1084.

USDA. (1986). *Urban Hydrology for Small Watersheds (TR-55)*. US Department of Agriculture.

Vogel, R. M., & Kroll, C. N. (1989). Low-flow frequency analysis using probability-plot correlation coefficients. *Journal of Water Resources Planning and Management, 115*(3), 338–357.

Wahyudi, et al. (2020). Dinamika Pertumbuhan Permukiman dan Risiko Banjir di Surakarta. *Jurnal Perencanaan Wilayah*, *8*(2), 112–125.

Weng, Q. (2021). Remote Sensing for Urban Sustainability. *Remote Sensing*, *13*(5), 1006.

Zhang, X., et al. (2021). Urban Land Cover Classification Using Sentinel-2. *Remote Sensing of Environment*, *254*, 112246.